Supplementary Material for Leveraging Visual Blur Perception Characteristics for EEG Decoding

Anonymous submission

Network parameters

The detailed parameters of the paper are shown in Table 1.In Blurring pipline we used Gaussian blurring for the input visual stimuli, and controlled the different blurring levels by controlling the size of the Gaussian kernel, in the experiments we chose the Gaussian kernel sizes ranging from 3 to up to 64, and sampling was performed every 6. The CLIP model of RN50 was chosen as the most visual coder, and the parameters of the model were obtained from OpenClip (Ilharco et al. 2021). In feature selection, a randomly initialized R matrix was used. The Things-EEG and Things-MEG datasets were used in the experiments for testing, and the same preprocessing as in the paper (Wu et al. 2025) was used for data preprocessing in order to make a fair comparison.

More comprehensive ablation experiments

We performed more comprehensive ablation experiments to verify the effects of Blurring pipeline, Feature adapter and Spatial Conv on performance. The results are shown in the Table2, from which it can be seen that removing any one of these modules results in a decrease in performance, while removing more modules results in a further decrease in performance, which further demonstrates the role of each module in performance improvement.

More visualization results

More EEG activation maps are shown in Figure 1 to demonstrate the generalizability of the paper's results.

More Generated Images

More results generated by EEG representation -guided generation are shown in Figures 3 and 2. We used the method proposed in paper (Li et al. 2024) for EEG-guided image generation. Specifically, we trained a simple diffusion model, used the EEG-extracted representations to generate the CLIP cue representations used by the SDXL+IP-Adapter (VIT-H-14), and then used the generated representations to guide image generation. This method leverages the powerful image generation capability of SDXL+IP-Adapter, which is superior in EEG-guided image generation. In this paper, we use this method as a data visualization method to demonstrate that some key information in visual stimuli, such as shape, color, orientation, and category of the subject, are retained in the extracted representations in the EEG encoder.

Confusion matrix

We also visualized the confusion matrix for each subject on the test set, as shown in Figure 4, from which it can be seen that most of the paired EEG representations and image representations can be matched well, with only a few samples being misclassified.

Comparison with other EEG encoders

To validate the effectiveness of the EEG Encoder used in this paper, we replaced the EEG Encoder with EEGNet(Lawhern et al. 2018), TSconv(Song et al. 2023), and EGProjectLayer(Wu et al. 2025) for comparison, with the results shown in Table 3. As can be seen from the table, the method proposed in this paper maintains the best performance compared to other methods, which demonstrates that the EEG Encoder used in this paper has a significant advantage over other methods in an EEG decoding framework based on visual blur perception characteristics.

Limitations

The method proposed in this paper adopts the method of aligning EEG representations and with visual representations for training, and the improvement of model performance also further proves that the brain has some of the same properties as the existing AI methods in performing visual processing processing, and this cross-modal alignment strategy not only provides new perspectives for understanding the mechanism of human visual perception but also provides ideas for the development of AI algorithms that are closer to biological intelligence provides ideas. In addition, this paper attempts to briefly explore the visual processing mechanism using the proposed method, however, the low signal-to-noise ratio and low spatial resolution of the EEG signal make it difficult to accurately parse the fine-grained representation patterns of the brain in visual tasks, and future studies may consider combining the high spatial resolution neuroimaging techniques such as fMRI or introducing more advanced signal denoising and feature enhancement algorithms in order to more accurately reveal the the neural mechanisms of visual information processing.

Table 1: Detailed parameters of the model.

Modules	Input	Output	Settings
Visual representation construction			
Blurring pipeline	(3,224,224)	(10,3,224,224)	cv2.GaussianBlur, kernel_sizes = [3,9,...,57,63]
Visual encoder	(10,3,224,224)	(10,1024)	CLIP(RN50)
Feature selection	(10,1024)	1024	R Weight matrix [10,1024]
Feature adapter (Linear 1)	1024	1024	torch.nn.Linear(1024, 1024)
Feature adapter (Linear 2)	1024	1024	torch.nn.Linear(1024, 1024)
EEG representation construction			
Spatial Conv	(1, 63,250)	(25,1,250)	torch.nn.Conv2d(25,(63,1))
Shared MLP(Linear 1)	(25,1,250)	(25,1,200)	torch.nn.Linear(250, 200)
Shared MLP(Linear 1)	(25,1,200)	(25,1,200)	torch.nn.Linear(200, 200)
Flatten	(25,1,200)	(5000)	-
EEG adapter(Linear)	(5000)	1024	torch.nn.Linear(5000, 200)

Table 2: More comprehensive ablation experiments.

Blurring pipeline	Feature adapter	Spatial Conv	Top - 1	Top - 3	Top - 5
✓			54.56±6.91	76.41±5.54	84.71±4.65
	✓		45.04±6.40	68.11±6.47	77.20±5.84
		✓	35.58±5.75	57.59±7.43	67.80±6.87
✓	✓		67.04±6.11	85.36±4.65	91.45±3.27
✓		✓	56.21±6.86	77.87±5.77	85.68±4.43
	✓	✓	57.27±5.09	79.91±4.83	86.95±4.18
✓	✓	✓	**80.00±4.19**	**93.92±2.30**	**96.89±1.43**

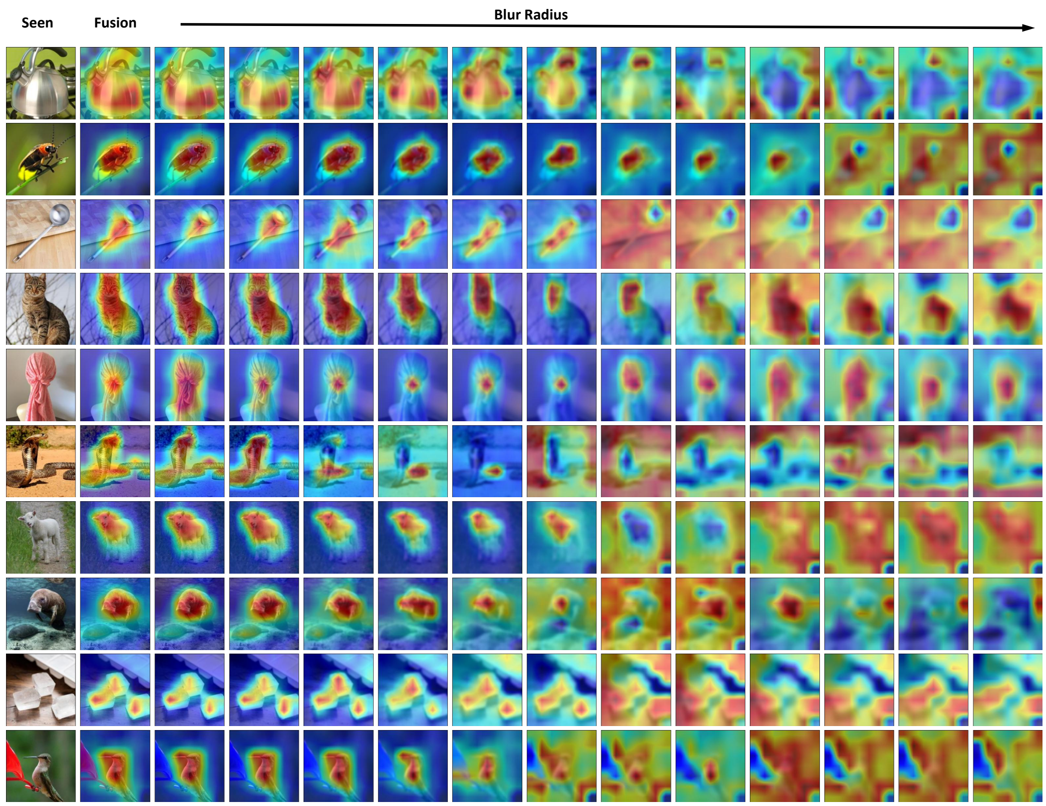

Figure 1: More results for EEG activation maps.

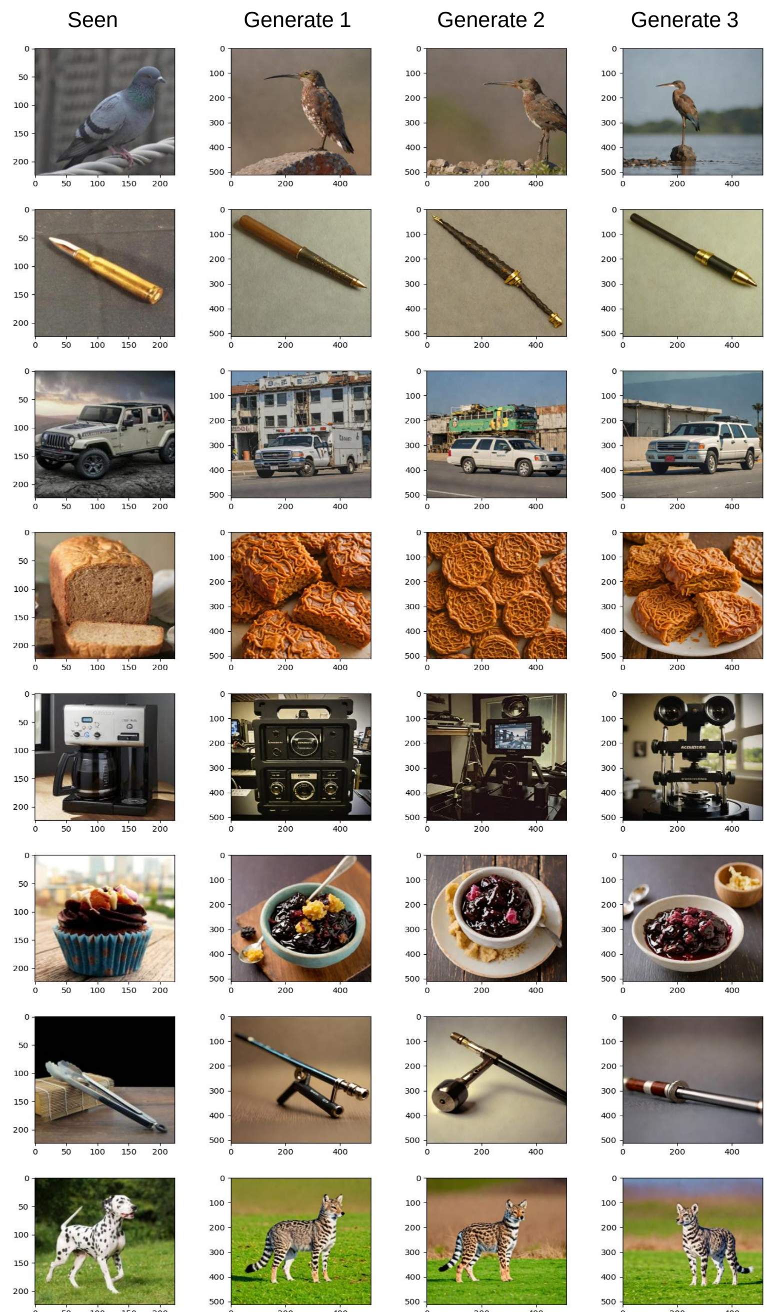

Figure 2: Additional Generated Images

Table 3: Comparison with other EEG encoders.

Methods	Top-1	Top-3	Top-5
EEGnet	56.96±5.79	79.54±4.57	86.74±3.34
TSconv	48.70±6.61	71.55±7.15	81.10±5.87
EEGProjectLayer	57.20±5.81	80.15±5.64	87.50±4.72
Ours	80.00±4.19	93.92±2.30	96.89±1.43

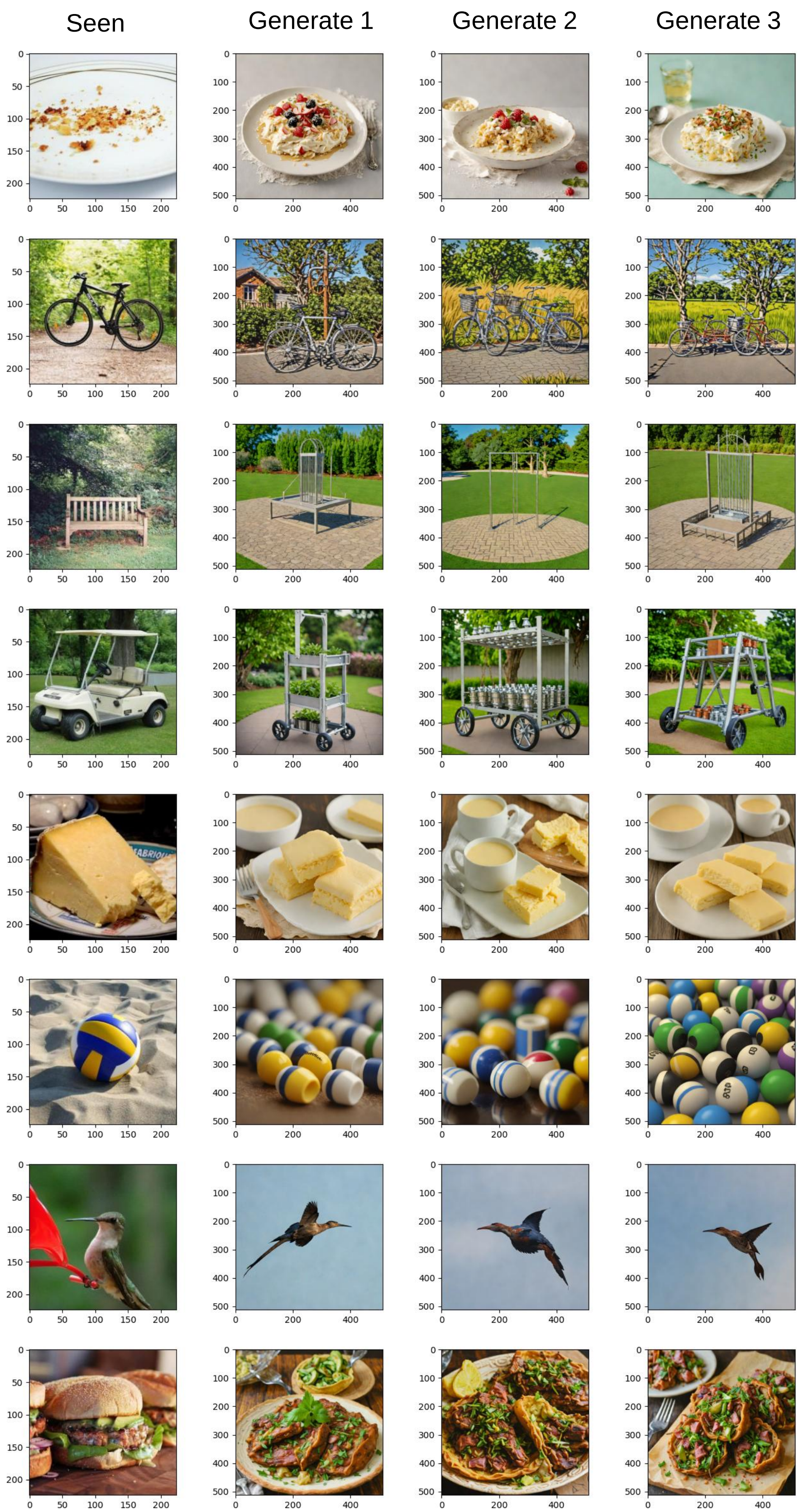

Figure 3: Additional Generated Images

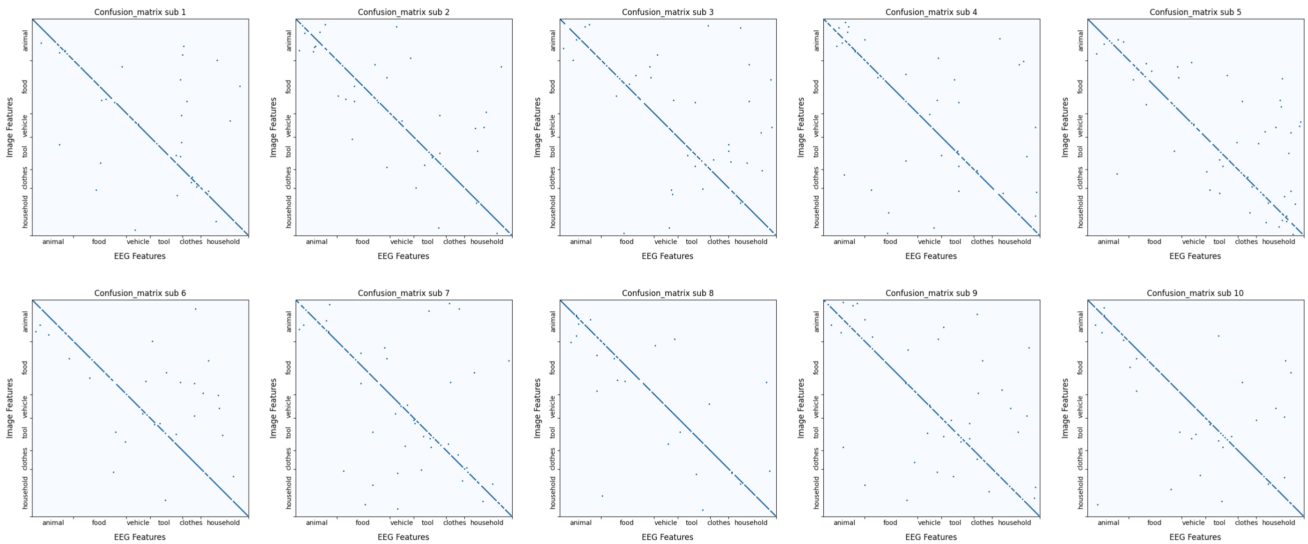

Figure 4: Confusion matrix for 9 subjects on the Things-EEG dataset.

References

Ilharco, G.; Wortsman, M.; Wightman, R.; Gordon, C.; Carlini, N.; Taori, R.; Dave, A.; Shankar, V.; Namkoong, H.; Miller, J.; Hajishirzi, H.; Farhadi, A.; and Schmidt, L. 2021. OpenCLIP. If you use this software, please cite it as below.

Lawhern, V. J.; Solon, A. J.; Waytowich, N. R.; Gordon, S. M.; Hung, C. P.; and Lance, B. J. 2018. EEGNet: a compact convolutional neural network for EEG-based brain–computer interfaces. *Journal of neural engineering*, 15(5): 056013.

Li, D.; Wei, C.; Li, S.; Zou, J.; Qin, H.; and Liu, Q. 2024. Visual decoding and reconstruction via eeg embeddings with guided diffusion. *arXiv preprint arXiv:2403.07721*.

Song, Y.; Liu, B.; Li, X.; Shi, N.; Wang, Y.; and Gao, X. 2023. Decoding natural images from eeg for object recognition. *arXiv preprint arXiv:2308.13234*.

Wu, H.; Li, Q.; Zhang, C.; He, Z.; and Ying, X. 2025. Bridging the Vision-Brain Gap with an Uncertainty-Aware Blur Prior. arXiv:2503.04207.